2020-11-08

Performance characteristics and permittivity modeling of a surface plasmon resonance sensor for metal surface monitoring in a synthetic maritime environment

Lavers, Chris

10.1117/12.2585161
SPIE Future Sensing Technologies
SPIE

Performance Characteristics and Permittivity Modelling of a Surface Plasmon Resonance Sensor for Metal Surface Monitoring in a Synthetic Maritime Environment

Christopher R. Lavers *[a], Dr AM Cree*[b], Dr D Jenkins*[b], Mr N Salah*[b], and Mr M Findlay*[b],
[a] Plymouth University at Britannia Royal Naval College, College Way, Dartmouth, Devon, TQ6 0HJ;
[b] Faculty of Science and Engineering, Plymouth University, Drake Circus, Plymouth, PL4 8AA, United Kingdom.

ABSTRACT

Surface Plasmon Resonance (SPR), an established optical sensing mode for providing quantified surface, is applied here to evaluate its suitability to provide optical parameters from metal layer measurements in a synthetic marine environment. We investigated silver noble metal films exposed to standard saline solution. Silver layers exhibit both long-term durability, and linear temporal reflectivity change, recorded in SPR minimum angle and SPR curve shape. Optical sensor design was achieved using Fresnel's optical theory for isotropic multi-layer media. We developed a data-fitting routine, providing numerical real and imaginary permittivity, and thickness solutions for corroded surfaces.

Keywords: Surface plasmon resonance, environmental sensing optical modelling

1. INTRODUCTION

We evaluate the suitability of Surface Plasmon Resonance (SPR) an established optical sensing technique to quantify surface permittivity parameters (real and imaginary permittivity, and thickness) for silver films exposed to a synthetic marine standard environment. Metal layers exhibit long-term durability, and linear temporal reflectivity change recorded in SPR angle and curves. Sensor design was achieved with Fresnel's optical theory for isotropic multi-layer media. We developed a data-fitting routine, yielding numerical permittivity, and thickness solutions for 'corroded ' surfaces.

Many attempts have been made to create accurate surface monitoring corrosion sensors which suffer from inability to detect corrosion at low levels before serious damage is done. Corrosion may occur in inaccessible undersea pipelines or enclosed areas; it is hard to predict where or when it will occur. Corrosion-related fracture detection with optical sensors is attractive as it *may* reduce fleet or offshore structure maintenance cost. Sensors for optical applications have included optical fibres [**1**] or ellipsometry [**2**] where thickness and refractive index, must be known, whilst SPR can determine both. SPR sensors provide vital surface optical parameters (both real and imaginary permittivity and thickness), or early corrosion change when corroded material removal may avoid costly structural repairs. SPR was used for aqueous sensing [**3**], with potential for corrosion-related detection. We present our patent SPR method for corrosion detection [**4**], evaluating the surface analytical technique to detect time dependent corrosion in thin films, and from data-fitting provide quantified permittivity values.

*christopher.lavers@plymouth.ac.uk ; phone +44 803 677218; fax +44 803 677015

1.1 Corrosion and mechanical damage- key failure modes for optical detection

Apart from lost lives or disasters, it is estimated global annual corrosion in on / off shore metal pipelines. cost is $2.5 trillion [**5**]. In the USA 1998-2017, 306 fatalities and 1259 injuries were related to oil, gas or hazardous fluid pipeline failure, costing > $8.1 billion. Corrosion-induced failure has become a key concern in maintaining pipeline integrity. Annually thousands of barrels of oil spill into seas from corroded pipes. Corrosion may go undetected until components fail, or are irreparably damaged, often catastrophically. In one particular instance in1992 a Guadalajara petrochemical pipeline exploded, killing 215 people, traced back to a corroded pipe. Fracture is a recognised metal failure mode, often occurring without warning. Corrosion may induce stress or strain concentration in surfaces. Work has studied corrosion effects on metals, but less investigation of optical properties in *thin* metal layers < 1 micron, prior to often rapid fracture. Fatigue and corrosion are key engineering issues with corrosion described as an oxidation reaction (pure metal removed and replaced by oxide). Oxide layers are often weaker and more brittle than pure metal, reducing performance, lifespan, and may cause structural failure.

2. THEORETICAL MODELLING

2. 1 Surface Plasmon Resonance Theory

Transverse Magnetic light may excite SPR at metal-dielectric interfaces. SPR are collective surface electron oscillations interacting with light. Otto [**6**], and Kretschmann [**7**] developed ways to achieve this, with the Kretschmann configuration used here and in previous work [**8-9**]. Surface corrosion may include changes to film thickness d, real / imaginary permittivity, εr and εi respectively; surface changes include change to εr and εi only, or filling changes [**10**]. Mechanical properties are determined by local microstructure / texture under deposition or treatment, impacting corrosion susceptibility. Here thin coatings are deposited on thick substrates. SPR is supported between media of opposite sign of real parts of dielectric constant with exponentially decaying fields into each media, sensitive to changes in metal or dielectric:

$$\varepsilon_{1\,\mathrm{real}} + \varepsilon_{2\,\mathrm{real}} < 0 \qquad (1)$$

where $\varepsilon_{1\,\mathrm{real}}$ and $\varepsilon_{2\,\mathrm{real}}$ are the respective real parts of metal and dielectric film permittivities. The SPR is highly localised to the interface with exponentially decaying fields into each medium, having enhanced sensitivity when compared with conventional Attenuated Total Reflection (ATR) reflectivity, to changes in the metal or dielectric optical dielectric tensors [18]. When SPR is excited with p-polarised light, the wave-vector between 2 semi-infinite media is given by:

$$k_z = k_{SPP} = \frac{\omega}{c} \times \left(\frac{\varepsilon_{1\,\mathrm{real}} \times \varepsilon_{2\,\mathrm{real}}}{\varepsilon_{1\,\mathrm{real}} + \varepsilon_{2\,\mathrm{real}}} \right)^{0.5} = \sqrt{\varepsilon_{\mathrm{glass}}} \times \frac{\omega}{c} \times \sin\theta \qquad (2)$$

where z is along the interface, ω angular velocity, ε_{glass} the dielectric constant, and θ the incident angle. The k_{SPP} wave-vector of the SPR is highly dependent on the optical properties of the materials close to the interface along which it propagates. This sensitivity is a product of the high electric field strength at this boundary. This field induces polarisation in the adjacent layers, hence the wave-vector is dependent on their permittivity. This high degree of sensitivity makes surface plasmon resonance a valuable technique for measuring accurately the properties of thin films close to a boundary supporting the resonance.

We modelled SPR coupling in FORTRAN by varying parameters, e.g. thickness, for optimisation. Our method calculates reflectivity as a function of incident angle for multi-layer media as a series of isotropic slabs of thickness below a wavelength. A scattering method **[11]** accounts for reflection / transmission coefficients at interfaces between media, coupling incoming fields with a stable matrix. (**fig 1.)** As demonstrated in **fig. 1**, the vectors a1 and b2 go into the matrix,

and a2 and b1 come out. The forward moving vector a and the backward moving one b, the vectors in media 1 at the interface, have the subscript 1, whilst the vectors in medium 2 have the subscript 2. The elements in the vectors are modal amplitudes. Writing all these together in matrix form, generates what is known as the scattering matrix S. The input of the scattering matrix is the incoming waves, and the output is the outgoing waves and is a more stable approach than that taken with the more traditional transfer matrix approach.

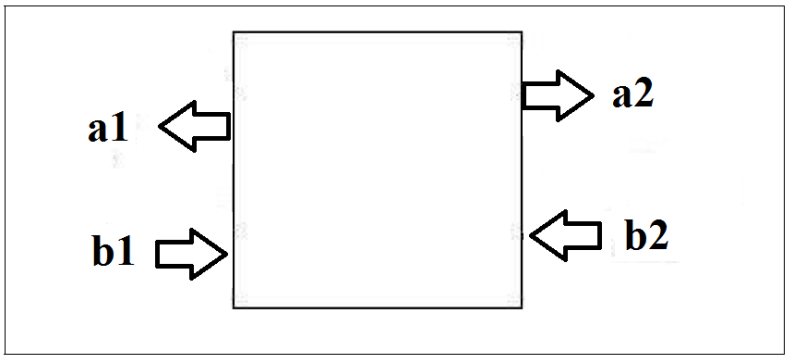

$$\begin{bmatrix} b_1 \\ a_2 \end{bmatrix} = S \begin{bmatrix} a_1 \\ b_2 \end{bmatrix} = \begin{bmatrix} R_1 & T^T \\ T & R_2 \end{bmatrix} \begin{bmatrix} a_1 \\ b_2 \end{bmatrix}$$

Fig 1. Scattering matrix approach.

Scattering matrix output is shown for a 4-layer 652nm simulation with 2000 angle steps, in **fig. 2.** Optical parameters are shown for a glass prism, chromium adhesion layer, silver, and air. SPR system modelling used film parameters taken from a recognised handbook **[12]**.

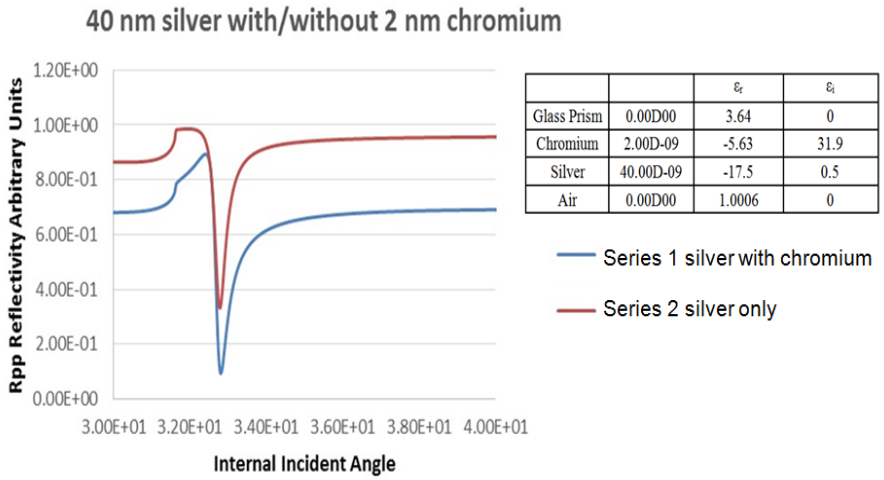

		ε_r	ε_i
Glass Prism	0.00D00	3.64	0
Chromium	2.00D-09	-5.63	31.9
Silver	40.00D-09	-17.5	0.5
Air	0.00D00	1.0006	0

Fig. 2 Theoretical SPR reflectivity plot for a typical silver film deposition.

3. EXPERIMENTAL METHOD AND MATERIALS

3.1 SPR Experimental Arrangement

In this work, we used the Kretschmann configuration to collect optical reflectivity from synthetic saline exposed samples over time (**fig. 3**). Thin metal films of firstly chromium, and then silver sputtered onto glass prisms. We used silver, but gold and copper may be chosen. Laser radiation was shone through the coupling prism so it was totally internally reflected above the critical angle. A vertically polarised (p-polarised) laser was stepped in angle under computer control until it coupled with the SPR resonance at the glass-metal interface, producing an evanescent wave along the surface. A helium-neon laser, at 632.8nm, provided the in-coupling laser light source. The frequency modulated chopper (Ealing) permits phase-sensitive detection (PSD) of both the signal and reference with lock-in amplifiers (EG&G), to minimise detected noise. The Analogue to Digital conversion and data acquisition takes place using a National Instruments USB 6210. A computer program, written in LabView, controlled the motorised rotation stage operation, and also recorded the photodiode reflectivities from both the sample and the reference beams. The motorised rotation stage allows the angle of incidence to be varied. The reflected light is detected by a silicon photodiode also mounted on the rotation stage. The two stages are linked by a gear system so that a θ movement of the prism table gives a 2θ turn of the photodiode; this ensures that the reflected beam always strikes the photodiode. As the rotation stages are moved by the stepper motor this generates a large set of data points, giving reflected intensity against a number of steps.

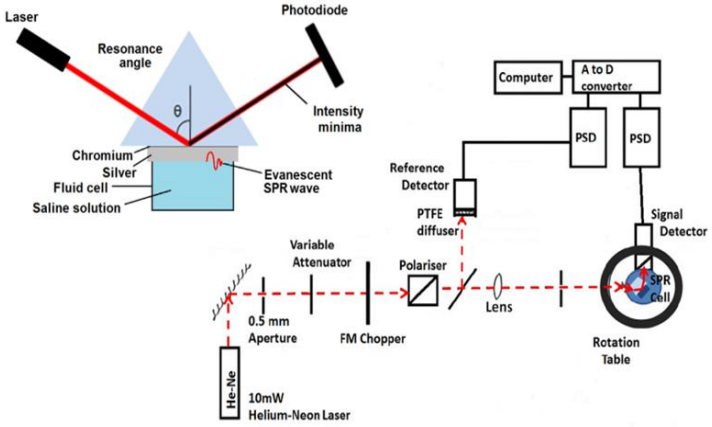

Fig. 3 Kretschmann SPR experimental configuration.

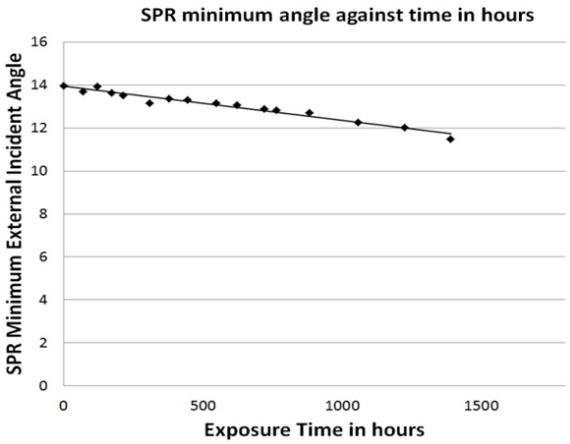

Fig 3a. Experimental SPR minimum reflectivity angle vs time in hours.

3. RESULTS AND DISCUSSION

4.1 Monitoring Surface Permittivity Changes of a Silver Layer

Before silver deposition, a thin chromium adhesion layer was sputter deposited. Group 1B metals (copper, silver, or gold) do not have strong adhesive properties to dielectrics like glass; such metals have low oxygen affinity. Hydroxyl groups on glass surfaces need oxide bonds to form strong adhesion. In order to achieve this we deposited an adhesion promoting layer of chromium (group VIa metal), nominally 2-3nm thick, onto the glass. Chromium forms covalent oxide bonds at surfaces with hydroxyl groups, promoting stronger adhesion. A 45nm silver film (±2nm) was then sputtered. High refractive index glass prisms were used. Silver was chosen from previous SPR work with this metal, as deposition rate and optimal thickness were known. The Plymouth University Nordiko 6" 50W sputterer achieved 6×10^{-7} mbar pressure, maintained by careful plasma tuning. SPR curves were taken with air, water or saline for theory *vs.* data. Cells show good stability over time, as with previous liquid crystal cells **[13]**. A Vernier Salinity Standard Sodium Chloride

Solution, nominally 35 parts per thousand, was added by syringe (0.8 ml) and sealed, halting cell evaporation. Reflectivity was recorded from a simulated marine environment, shown here for a silver film, **fig. 4**, for 2 months of continuously acquired data, with a downward angle trend in SPR resonant reflectivity minima after 1389 hours of synthetic saline solution exposure (**fig 3a**.). If the external prism angle is plotted as a function of time, in **fig. 3a**, a very good linear statistical correlation is seen (R^2 = 0.961), with a minimum angle, $\theta_{SPR\ minimum}$, altering over time according to a simple equation is found: $\theta_{SPR\ minimum}$ = - 0.0016t+13.953, with t the saline exposure time in hours. $\theta_{SPR\ minimum}$ results changed little and inconsistently over day 1, indicative of initial surface filling change, rather than film corrosion, or layer delamination [**14**].

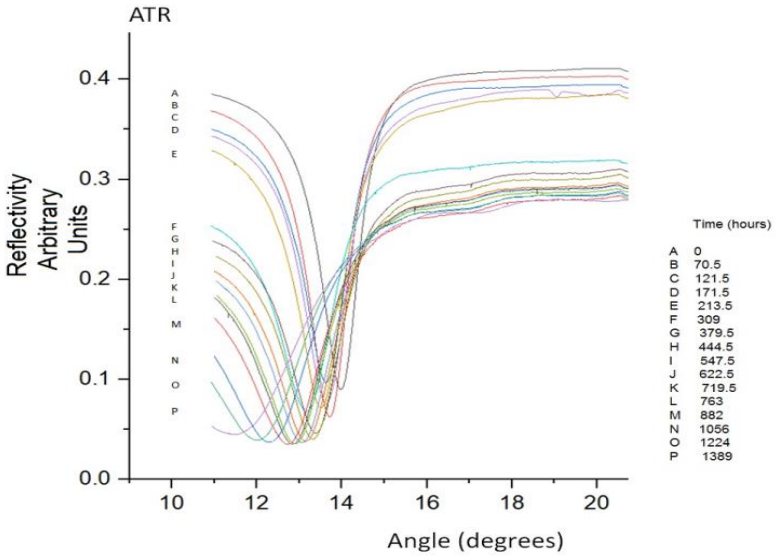

Fig. 4 SPR Experimental angle scans.

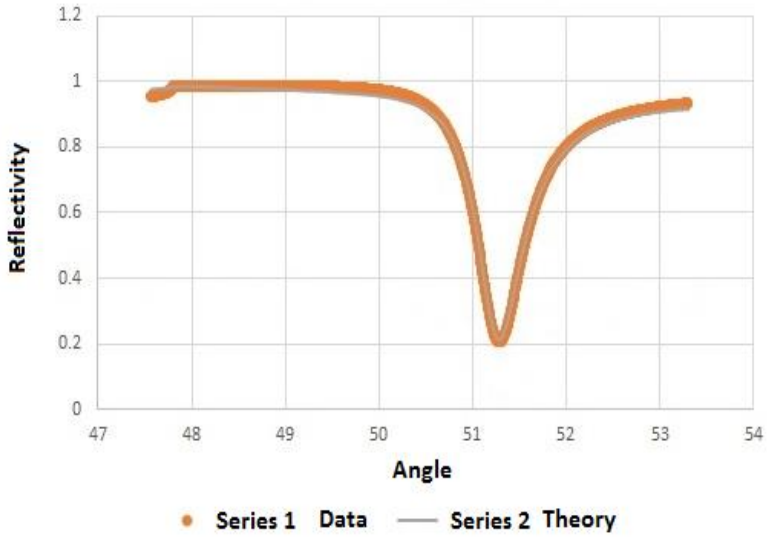

Fig. 5. SPR theoretical predictions fitted with experimental data.

4.2 Fitting Experimental Data

The technique minimises differences between recorded experimental data and theoretical predictions, varying the three parameters to achieve a theory curve matching experimental data. Parameters iterative to minimise mean square error σ^2 where:

$$\overline{\sigma^2} \quad = \quad \sum(R_i^t \; - R_i^e)^2 \quad (3)$$

$R^t{}_i$ is the theoretical reflectivity at the ith measurement angle and $R^e{}_i$ is the experimental reflectivity at the same angle. Iterative steps are chosen by a method of swiftest descent. Partial derivatives were calculated with respect to each of the parameters and the next search point in a direction opposed to the vector of the 3 derivatives where:

$$\begin{pmatrix} \epsilon' \\ \epsilon'' \\ t_l \end{pmatrix}_{i+1} = \begin{pmatrix} \varepsilon' \\ \varepsilon'' \\ t_l \end{pmatrix}_i - s \begin{pmatrix} \frac{\delta\overline{\sigma^2}}{\delta\epsilon'} \\ \frac{\delta\overline{\sigma^2}}{\delta\varepsilon''} \\ \frac{\delta\overline{\sigma^2}}{\delta t_l} \end{pmatrix} \quad (4)$$

i is the *ith* parameters' estimate, *s* the step length to the next estimate to achieve the least mean square error at the next point. Silver data vs minimised theoretical reflectivity is shown, **fig. 5** for a cell with permittivity: -18.47 + i0.33, and a 0.9nm silver oxide (AgO) layer, agreeing with other workers [**15**]. After an initial bulk 'free-fit' to fresh cell data allowed a 0.9 nm layer to 'free-fit' real / imaginary permittivity until the routine found a new minimum. De Rooij showed linear oxide thickness increased over time from an initial baseline value of 0.9 nm; his data agrees with observed linear angle shifts. Fits were obtained 0 – 267 minutes after filling. Fitted permittivities settle down over time (**fig. 6a**, **fig. 6b** respectively) displaying the complex unstable nature of 'corroded' metal. One such fit during day 2 is shown in **fig. 6c**.

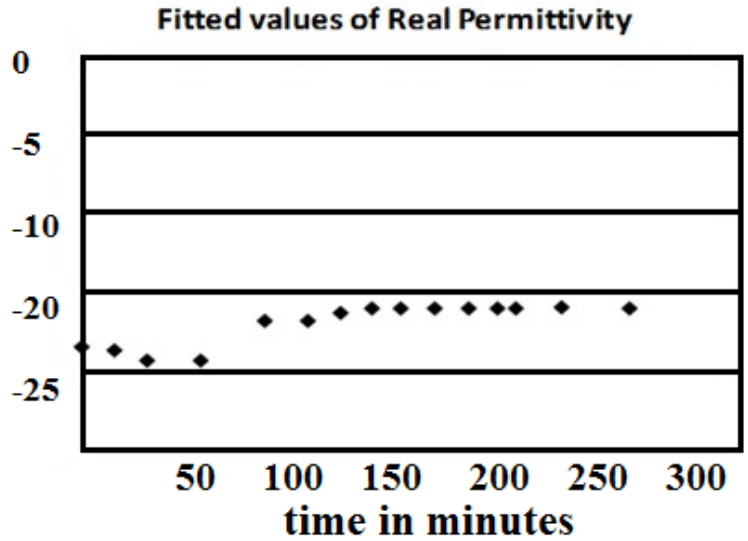

Fig. 6a Real permittivity.

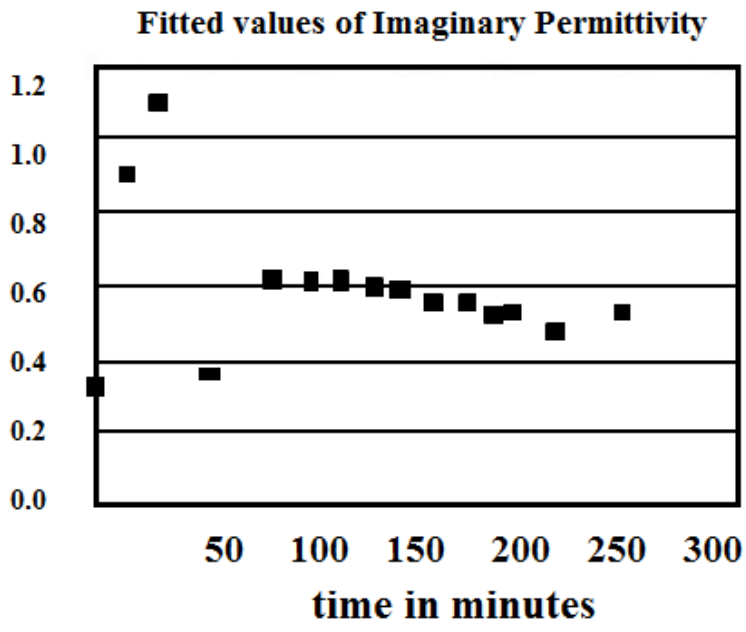

Fig. 6b Imaginary permittivity.

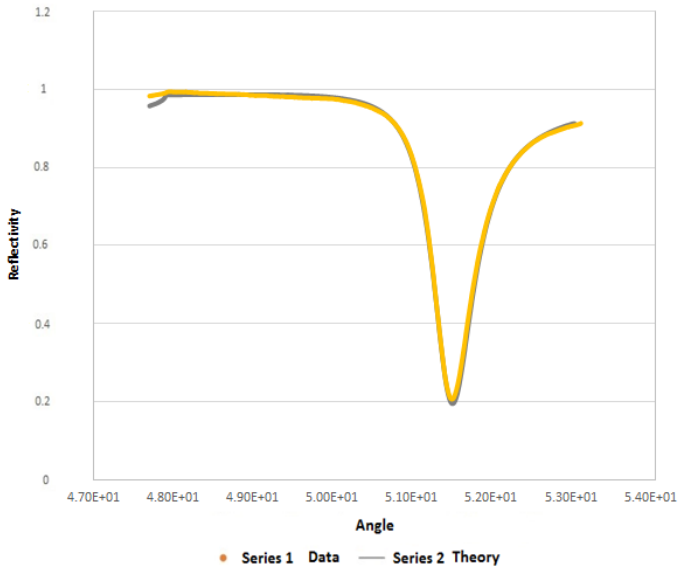

Fig. 6c Reflectivity vs data fit with permittivity and oxide thickness parameters respectively: -16.012438, 0.476319, 0.270821E-08.

Some SPR workers explain surface permittivity temporal variations due to solvent molecules entering a metal [**16**] resulting in composite metal / electrolyte film with different permittivity. Multiple oxide layers may grow into films, or water penetrate metal through voids, altering properties. Silver oxidation is limited to water / air diffusion, this is not a flow, cell, so no stirring occurs. Agitation *may* improve mass transfer to silver electrodes but likely disrupts polarisation. As we wanted to quantify static tank surface changes rather than flow pipes this was regarded unnecessary. Data acquisition was extensive, we obtained 35k cell data points, besides references.

5. CONCLUSIONS

SPR reflectivity minima measurements were plotted over time, and showed good linear correlation with angular dependence. The observed linear SPR coupling minima shift was as might be expected from a linear silver oxide increase shown by Rooij [**15**]. 'Immediate' Day 1 fitted results indicate surface filling changes rather than metal corrosion, or thickness loss, as films were still intact after 6 months. Observed reflectivity changes were large, there is nearly a 40% change in relative relativity between day 1 and day 2, with an approximately one degree shift in the position of the surface plasmon resonance minimum angle over this time. The SPR method provides quantified values for surface metal permittivities in a synthetic marine corrosive environment prior to fracture measurements, and also provides, in principle, an optical method for non-destructive evaluation monitoring of oxide growth rate.

Acknowledgements
Dr Paul Tiltman of the Research and Innovations Team for support with the initial SPR work and patent application.

6. REFERENCES

[1] Himour, A., Abderrahmane, S., Beliardouh, N.E., Zahzouh, M., Ghers, M., *Japanese Journal of Applied Physics*, 44(1), pp.305-10, (2005).
[2] Tompkins, H., *Handbook of Ellipsometry*, ISBN-13: 978-0815514992, William Andrew, (2005).
[3] Salah, N.H., Surface Plasmon Resonance Sensing and Characterisation of Nano-Colloids for Nanotoxicology Applications, PhD, Plymouth University, (2015).
[4] Lavers, C.R., *Optical SPR Sensor for Corrosion Patent Applications*, British Patent Application No. 1611929.9, (2016).
[5] Raising Awareness about Corrosion and Corrosion Protection around the World, *http://corrosion.org/* (accessed 31-10-2019).
[6] Otto, A., *Z Phys* 216, pp. 398-410, (1968).
[7] Kretschmann, E., and Raether, M., *Z.Naturf.*, 23(A), pp. 2135-36, (1968).
[8] Lavers, C.R., *Thin Solid Films*, 230, 217-224, (1993).
[9] Lavers, C.R., Jenkins, D., Cree, A., Salah, N., Findlay, M., *Proceedings of Sensors and Their Applications 18*, QMUL London, (2016).
[10] Maxwell-Garnett, J.C., *Phil Trans* A203, 385, (1904).
[11] Ko, D.Y.K., and Sambles, J.R., *J. Opt., Am.*, 5, p. 1863, (1988).
[12] Adachi, S., *The Handbook on optical constants of metals*, ISBN: 978-981-4405-94-2 World Scientific, (2012).
[13] Innes, R.A., and Sambles, J.R., *Optics Commun.*, 64, 288, (1987).
[14] Suresh, S., *Fatigue of Materials*, ISBN 0521570468 Cambridge University Press, 2004.
[15] Rooij, A. de, *ESA Journal*, Vol. 13, pp.363-382. (1989.
[16] Pollard, J.D., Sambles, J.R., and Bradberry, G.W., *J. Mod. Optics*, Vol. 37, pp. 841-846, (1990).